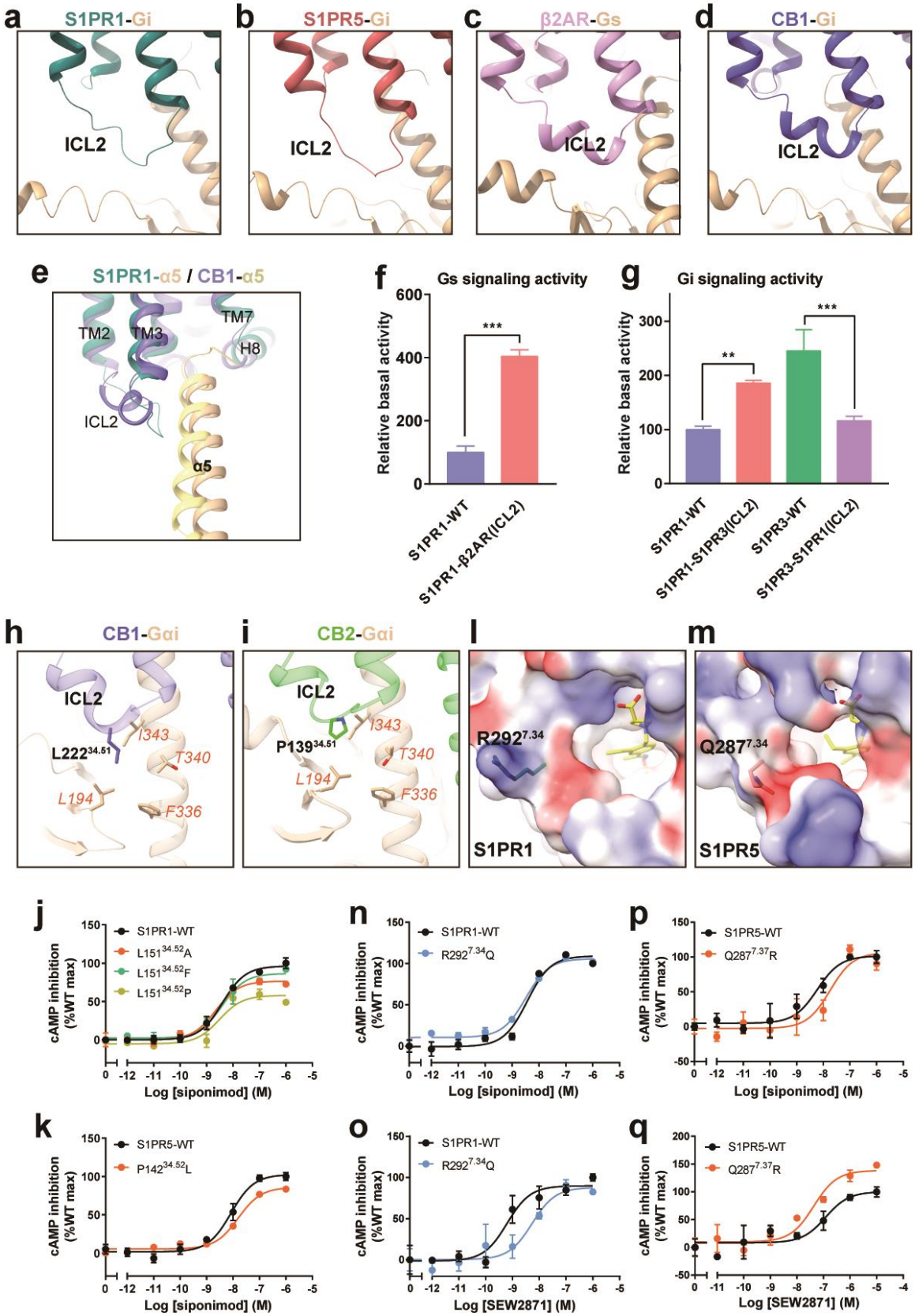
a
S1PR1-Gi
ICL2
b
S1PR5-Gi
ICL2
c
β2AR-Gs
ICL2
d
CB1-Gi
ICL2
e
S1PR1-α5 / CB1-α5
TM2
TM3
TM7
H8
ICL2
α5
f
Gs signaling activity
Relative basal activity
600
400
200
0
***
S1PR1-WT
S1PR1-β2AR(ICL2)
g
Gi signaling activity
Relative basal activity
300
200
100
0
**
***
S1PR1-WT
S1PR1-S1PR3(ICL2)
S1PR3-WT
S1PR3-S1PR1(ICL2)
h
CB1-Gαi
ICL2
I343
L222^34.51
T340
L194
F336
i
CB2-Gαi
ICL2
I343
P139^34.51
T340
L194
F336
l
R292^7.34
S1PR1
m
Q287^7.34
S1PR5
j
S1PR1-WT
L151^34.52A
L151^34.52F
L151^34.52P
cAMP inhibition (%WT max)
Log [siponimod] (M)
k
S1PR5-WT
P142^34.52L
cAMP inhibition (%WT max)
Log [siponimod] (M)
n
S1PR1-WT
R292^7.34Q
cAMP inhibition (%WT max)
Log [siponimod] (M)
o
S1PR1-WT
R292^7.34Q
cAMP inhibition (%WT max)
Log [SEW2871] (M)
p
S1PR5-WT
Q287^7.37R
cAMP inhibition (%WT max)
Log [siponimod] (M)
q
S1PR5-WT
Q287^7.37R
cAMP inhibition (%WT max)
Log [SEW2871] (M)

Figure S8. The interaction of the ICL2 with Gi protein, and functional assays for ligand selectivity in both S1PR1 and S1PR5.

(a-d) Structural comparison of ICL2 regions of S1PR1(teal), S1PR5 (Indian red), β_2AR (plum) and CB1(slate blue) with G protein complexes reveals the unique conformation in S1PR.

(e) Structural superposition of S1PR1-Gαi (teal, S1PR1; tan, Gαi) and CB1-Gαi (slate blue, CB1; khaki, Gαi) when aligning on the receptor.

(f-g) Basal activity of G protein signaling of S1PRs. The basal activity of Gs signaling of wide-type S1PR1 and S1PR1-β2AR(ICL2) chimeras (f). The basal activity of Gi signaling of S1PR1, S1PR1-S1PR3(ICL2), S1PR3 and S1PR3-S1PR1(ICL2) (g). Bar represents difference in calculated relative basal activity of G protein signaling of chimeras to each WT. ns, no significance, $^{**}p < 0.01$, $^{***}p < 0.001$ (one-way analysis of variance [ANOVA] followed by the Dunnett's test, compared with the response of WT). Data represent mean ± SEM from three independent experiments performed in triplicate.

(h-i) The detailed interaction of $L222^{ICL2/34.51}$ in CB1(slate blue) with the residues $L194^{G.S3.01}$, $I343^{G.H5.15}$, $T340^{G.H5.12}$, $F336^{G.H5.08}$ in Gαi, as well as $P139^{ICL2/34.51}$ in CB2(lime) with the residues $L194^{G.S3.01}$, $I343^{G.H5.15}$, $T340^{G.H5.12}$, $F336^{G.H5.08}$ in Gαi. Residues from α5 are shown in orange font. The residues belonging to S1PR1 are shown in black font.

(j-k) Effects of the $L151^{ICL2/34.52}$A, $L151^{ICL2/34.52}$P, $L151^{ICL2/34.52}$F mutation of S1PR1 (j) and $P142^{ICL2/34.52}$ mutation of S1PR5 (k) on siponimod induced cAMP inhibition. Data are presented as the mean ± SEM of three independent experiments performed in triplicate.

(l-m) Surface representation of charge property of S1PR1 (l) and S1PR5 (m) colored according to their electrostatic charge.

(n-o) Effects of the $R292^{7.34}$Q mutation of S1PR1 on Siponimod (n) and SEW2871 (o) induced cAMP inhibition. Data are presented as the mean ± SEM of three independent experiments performed in triplicate.

(p-q) Effects of the $Q287^{7.34}$R mutation of S1PR5 on siponimod (p) and SEW2871 (q) induced cAMP inhibition. Data are presented as the mean ± SEM of three independent experiments performed in triplicate.